Semiconductor Physics, Quantum Electronics & Optoelectronics. 1999. V. 2, N 1. P. 133-141.

PACS 42.55.L, 42.60.P, 42.62

Iodine-stabilized He-Ne laser pumped by transverse rf-discharge

O. V. Boyko, A. M. Negriyko, L. P. Yatsenko

Institute of Physics, National Academy of Sciences of Ukraine, Kyiv, 252028, Ukraine,
tel. 265-14-80., fax 265-09-72,
e-mail: boyko@iop.kiev.ua, negriyko@iop.kiev.ua, yatsenko@iop.kiev.ua

Absrtact. The results of experimental investigations of He-Ne/$^{127}I_2$ lasers (λ = 633 nm) pumped by transverse rf-discharge are presented. Due to the low level of amplitude fluctuations, the frequency stability of such lasers reaches $5\cdot10^{-13}$ for the integration time 100 s, and it is about six times as large as the stability of the lasers pumped by dc-discharge. The modulation shifts of the frequency of stabilized He-Ne/$^{127}I_2$ lasers were measured with high accuracy in the wide range of the frequency deviation 1.5 MHz $\leq D \leq$ 20 MHz. The sources of the asymmetry of saturated-absorption resonances were determined as the joint action of the lenslike properties of the absorption medium and the elastic velocity-changing collisions of absorbing molecules. The results of a bilateral laser frequency comparison of the developed laser and the laser DE-3 (KIM, Kharkiv) are reported.

Keywords: He-Ne laser, freqency shift, frequency stabilization, resonance asymmetry.

Paper received 26.02.99; revised manuscript received 07.04.99; accepted for publication 19.04.99.

1. Introduction

For the practical realization (*mise en pratique*) of the definition of the metre as the length of the path traveled in vacuum by light in 1/299792458 s [1] *Comité International des Poids et Mesures* recommended twelve standard wavelengths in 1997 [2]. In particular, the wavelengths of He-Ne laser stabilized to hyperfine structure (HFS) components of the *R*(127) absorption line of vibration band 11-5 of $B^3\Pi_u^+ \leftarrow X^1\Sigma_g^+$ transition of $^{127}I_2$ molecule are very important for practical applications.

In spite of wide use of the He-Ne lasers in the metrology, a number of important physical questions remains so far uncertain including the origin of the so called modulation shifts, which are the main factors limiting the frequency reproducibility of the stabilized He-Ne/$^{127}I_2$ lasers. Usually, to obtain an error signal, the laser frequency is modulated with the deviation *D* at the frequency *f,* and the third harmonic of this frequency is detected in the output power. The servo-system holds the laser frequency at the value, for which the third harmonic amplitude is zero. It turned out [3] that the frequency location of the third harmonic zero substantially depends on *D*, which results in the shifts of the stabilized laser frequency when *D* changes (modulation shift).

If the servo-system is perfect, it is the asymmetry of the saturation absorption resonance used as the frequency reference that can give rise to the modulation shifts. The lenslike properties of the absorption medium related with the radial inhomogeneity of the laser intensity, which results in the inhomogeneous saturation of the absorption medium dispersion are considered in Ref. [4–7] as the cause of this asymmetry. Another way was proposed in Ref. [8] where the saturated absorption reso-

nances asymmetry due to velocity-changing collisions of absorbing molecules was considered. To determine the relative role of these mechanisms one can use the dependence of the stabilized laser frequency on the deviation D which has to be nonlinear and to be considerably different for various models of the asymmetry. However, it was impossible to answer this question up to now because this dependence was measured only in the narrow range 3 MHz $\le D \le$ 10 MHz, where it was linear. Thus, the experimental measurements of the modulation shifts in more wide range of the deviations D with the higher accuracy will let to specialize the real mechanism of the asymmetry of the saturated absorption resonances in the He-Ne/$^{127}I_2$ lasers.

Usually, for the frequency stabilization, He-Ne lasers pumped by dc-discharge (DCD) are used [9,10]. Meanwhile, it is well known that the first He-Ne lasers were pumped by longitudinal rf-discharge (RFD). However, these lasers had considerable disadvantages such as local overheat of the laser tube near the electrodes, what reduces its time of life; high level of rf-power, which is necessary for sufficient inversion making; considerable longitudinal inhomogeneity of the discharge, etc. Because of these disadvantages, such lasers were replaced by lasers pumped by DCD, which are more convenient for use and have longer time of life. In turn, these lasers have a number of considerable disadvantages such as high working voltage, the internal electrodes, the excitation of the various plasma oscillations, the separation of the components of the gain mixture in space, the longitudinal drift of the working atoms, etc. It is possible to avoid most of them by using the transverse RFD.

Moreover, the transverse RFD provides in He-Ne lasers more uniform distribution of the gain and increases the gain of the laser active medium. The optimum pressure of the gain mixture in the transverse RFD is higher then in the DCD, which increases both the resources of such lasers and the output power. The charged particles longitudinal drift and the separation of the components of the mixture are not observed in the RFD due to both the high frequency of the exciting field oscillations and their transversity [11-13].

It is the practically absence of low-frequency plasma oscillations that is the important preference of the transverse RFD in He-Ne lasers. As result, the level of the amplitude fluctuations in such lasers is lower then in lasers pumped by DCD. Hence, the use of the RFD in the stabilized He-Ne/$^{127}I_2$ lasers can increase considerably both the frequency stability and the accuracy of measurements of the frequency shifts.

The experimental setup is described in the Sec. 2. The results of the measurements of the He-Ne/$^{127}I_2$ laser frequency stability are reported in Sec. 3. The analysis of the modulation shifts measured in the deviation range 1.5 MHz $\le D \le$ 20 MHz and discussion of the causes of the resonance asymmetry is given in Sec. 4. The results of a bilateral laser frequency comparison between developed laser and laser DE-3 (KIM, Kharkiv) is presented in the Sec. 5.

2. Experimental setup

The laser layout is shown in Fig.1. For high passive stability, the 45 cm long laser cavity is formed by three invar rods. The 22 cm long commercial laser tube pumped by transverse RFD (from laser LGI-201) and the 6.5 cm long iodine cell filled by $^{127}I_2$ are mounted on holders, which are fastened on the invar rods. The first mirror R1 has 2 m radius of curvature and 99.8 % reflectivity. The output mirror R2 of 1 m radius of curvature and 99 % reflectivity is mounted on a piezoelectric transducer (PZT). For decreasing influence of flows of the ambient air, the space between all elements of laser is sealed

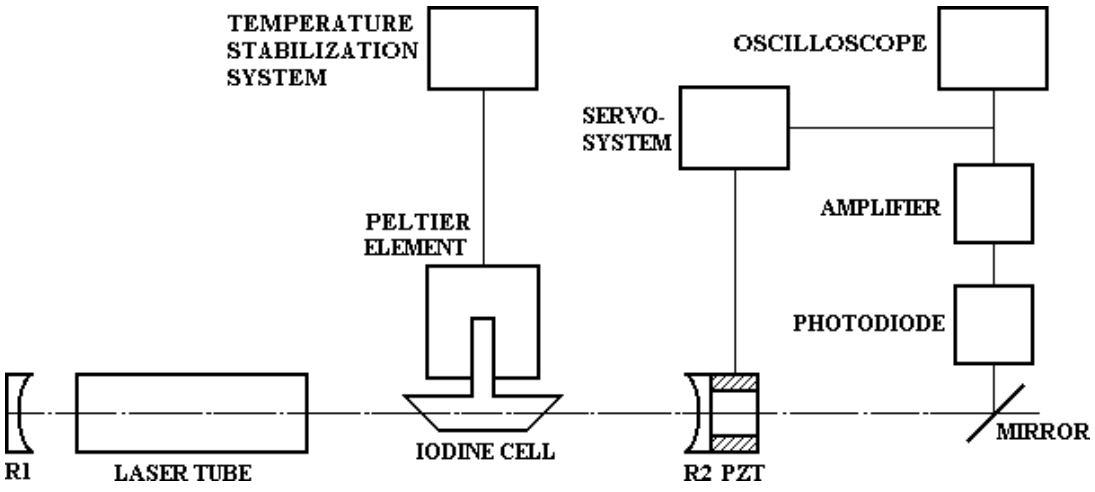

Fig. 1. Laser layout.

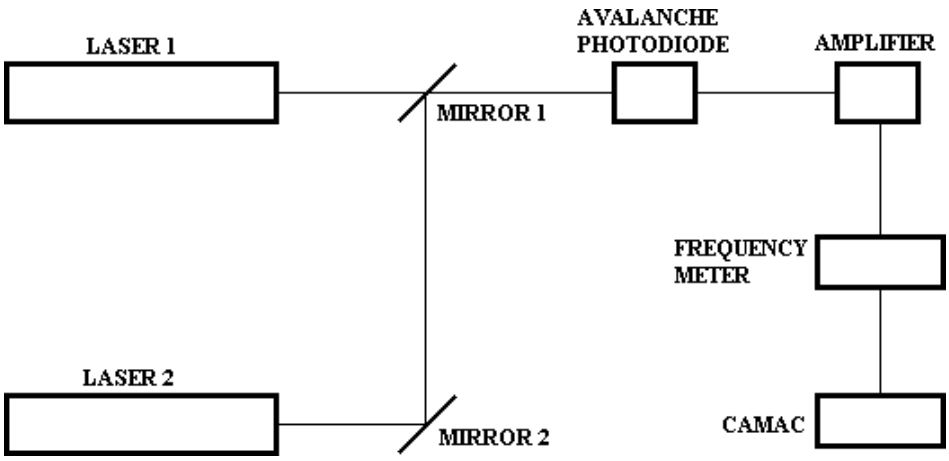

Fig. 2. Experimental setup.

against the surroundings and the setup is enclosed by special enclosure. The iodine cell finger is thermoelectrically cooled by the Peltier element in order to control the iodine vapor pressure. The temperature stabilization system controls the temperature in the range from 0°C to the room temperature within ±0.01°C.

The laser frequency is modulated by the sine voltage, which is applied to PZT. The servo-system stabilizes the mean frequency of the laser by locking on the saturated absorption components *d*, *e*, *f*, *g*, *h*, *i* and *j* of the HFS components of the *R*(127) absorption line of the 11-5 vibration band of the $B^3\Pi_{ou}^+ \leftarrow X^1\Sigma_g^+$ transition of the $^{127}I_2$ molecule. The stabilization is realized by use the well-known third-harmonic technique.

The experimental setup is shown in Fig. 2. The lasers 1 and 2 have above-mentioned design. The laser beams are brought together on the avalanche photodiode for the difference between optical frequencies of the lasers detection.

3. Frequency stability

The frequency spectra of the amplitude noise of the laser pumped by DCD and the laser pumped by RFD were measured for equal laser intensities. They are shown in Fig. 3 (the curve 1 and 2, respectively). The frequency spectrum of the dark noise of the photodiode is shown too (the curve 3). One can see that the noise of the laser pumped by DCD is larger than one of the laser pumped by RFD. Their ratio reaches four in the actual frequency range 1–5 kHz where the servo-system is operating.

The relative frequency stability of the lasers pumped by RFD was measured in terms of the standard Allan variance:

$$\sigma(2,\tau) = \frac{1}{\nu}\sqrt{\frac{\frac{1}{2}\sum_{i=1}^{N}\left(f_i - f_{i-1}\right)^2}{2\,(N-1)}}, \qquad (1)$$

where τ is the integration time, f_i is the measured beat frequency between the two lasers, ν is the frequency of laser radiation, N is a number of measurements of the beat frequency.

The measured $\sigma(2,\tau)$ for lasers pumped by RFD is

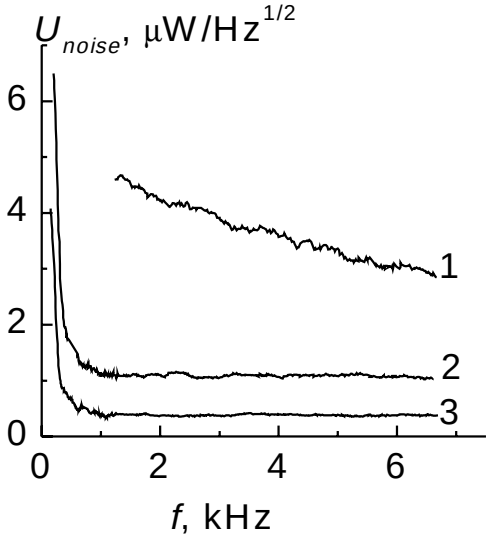

Fig. 3. Spectra of amplitude noise of the laser pumped by DCD (curve 1) and the laser pumped by RFD (curve 2). Curve 3 is the dark noise of the photodiode.

shown in Fig. 4 (curve 1). The curve 2 shows $\sigma(2,\tau)$ for lasers pumped by DCD. The latter one was obtained with the same servo-systems at the similar conditions (the iodine pressure was p = 20 Pa, the frequency deviation was D = 6 MHz) [14]. One can see that the stability of lasers pumped by RFD is about six times higher then one of the lasers pumped by DCD.

4. Modulation shifts and the asymmetry of the saturated absorption resonances

As it was pointed out, the stabilized laser frequency depends on the deviation D due to the asymmetry of the saturated absorption resonances. It is possible to determine the relative role of different sources of the resonances asymmetry if this dependence is known in wide range of deviation. The most important sources are lens-like properties of the absorbing medium and the elastic velocity-changing collisions of absorbing molecules.

4.1. Lens effect

It is well-known [4-7] that the frequency dependent part ΔP of the output power of the laser with intracavity absorption (the saturated absorption resonance shape) near the central frequency ω_g of the absorption line is the sum of symmetrical and antisymmetrical relative to detuning $\Delta\omega = \omega - \omega_g$ terms

$$\Delta P = kP_0\left(L_s\left(\Delta\omega/\Gamma\right) - \chi_{lens} L_a\left(\Delta\omega/\Gamma\right)\right), \quad (2)$$

where k is the resonance contrast, ω is the laser frequency, Γ is the absorption homogeneous linewidth. For the weak saturation of the absorption, the form-factors $L_s(x)$ and $L_a(x)$ are the real and the imaginary parts of the complex Lorentzian $L(x) = 1/(1+ix)$, respectively:

$$L_s(x) = \mathrm{Re}\left\{L(x)\right\} = \frac{1}{1+x^2}, \quad (3)$$

$$L_a(x) = \mathrm{Im}\left\{L(x)\right\} = -\frac{x}{1+x^2}. \quad (4)$$

The small parameter χ_{lens} describes the role of the intracavity spatial inhomogeneity. In the case of the weak saturation of the gain it is the sum of three factors. Each factor reflects the relative contribution for different ways of the nonlinear lenslike properties of absorbing medium influence on the output power [15]:

$$\chi_{lens} = \varepsilon \frac{\Delta\omega_p \eta}{\delta\omega_a} K_g - T_d \ln\frac{1}{T_d} K_d - 2\frac{\Delta\omega_p(\eta-1)}{\delta\omega_a} K_V, \quad (5)$$

where $\Delta\omega_p$ is the frequency bandwidth of the cavity, η is the ratio of the pump to its threshold value, $\delta\omega_a$ is the frequency interval between axial modes, T_d is the diffraction losses per one trip. The small parameter ε describes the radial inhomogeneity of the linear gain $g(r)$, which is approximated by $g(r) = g_0(1 - \varepsilon r^2/w_0^2)$, where g_0 is the linear gain on the gain tube axis, w_0 is the Gaussian beam waist radius. The dimensionless factors $K_i \sim 1$ in (5) are determined by the cavity geometry. Their explicit expressions can be find in the [15]. The first and the third terms describe the effective gain coefficient change, which concerned with linear $\varepsilon \neq 0$ and nonlinear $\eta - 1 \neq 0$ gain inhomogeneities. The second term arises due to the diffraction losses dependence on the Gaussian beam radius on the bounding aperture.

One can see from (5) that the level of the asymmetry depends on a number of parameters. It is difficult to find the χ_{lens} as long as the values of these parameters are usually unknown. One can use the dependence of the modulation shift $\Delta\Omega$ on the deviation D for the determination of the lens effect contribution to the resonance asymmetry. The quantity $\Delta\Omega$ is defined as the detuning $\Delta\omega$ corresponding to the third harmonic zero

$$S_3(\Delta\Omega) = 0, \quad (6)$$

where

$$S_3(\Delta\Omega) = \frac{f}{2\pi}\int_0^{2\pi/f} \Delta P\left(\Delta\omega + \frac{D}{2}\cos(ft)\right)\cos(3ft)\,dt. \quad (7)$$

Using (2), the solution of the equation (6) for the case of small asymmetry can be written as

$$\Delta\Omega = \chi_{lens} \frac{1+m^2}{1+3\sqrt{1+m^2}}\Gamma, \quad (8)$$

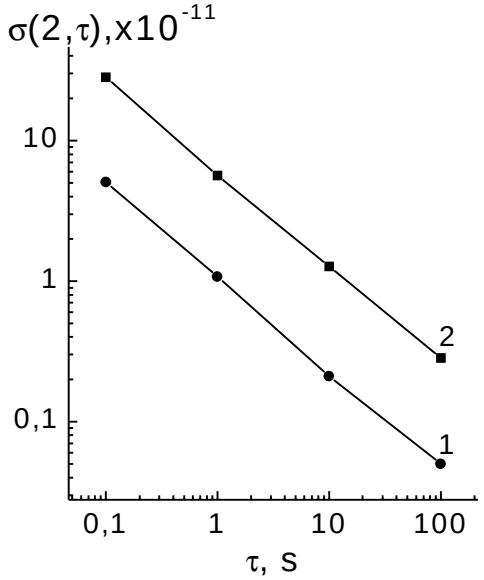

Fig. 4. Dependencies of the Allan variance $\sigma(2,\tau)$ on the integration time for laser pumped by RFD (curve 1) and laser pumped by DCD (curve 2).

where $m = D/2\Gamma$.

4.2. Elastic velocity-changing collisions of absorbing molecules

As it was shown in the Ref. [8], the elastic velocity-changing collisions of absorbing molecules can cause the asymmetry of the saturated absorption resonances. For the weak saturation of the absorption, the resonance shape can be written as [8]

$$\Delta P = kP_0\left(L_s(\Delta\omega/\Gamma) - \chi_{coll} L_a(\Delta\omega/\Gamma)\right), \tag{9}$$

where the form-factor $L_s(x)$ is the real part of the complex Lorentzian $L(x)=1/(1+ix)$ and is defined by (3), the $L_a(x)$ is

$$L_a(x) = \mathrm{Im}\left\{L(x)^4\right\} = -\frac{x(1-x^2)}{(1+x^2)^4}. \tag{10}$$

The small parameter χ_{coll} is determined by expression

$$\chi_{coll} = \frac{\nu_{12}''}{\Gamma}\left(\frac{\Delta\omega_D\theta_0}{\Gamma}\right)^2, \tag{11}$$

where the complex parameter ν_{12} is the frequency of elastic collisions for the nondiagonal element of the absorbing gas density matrix, $\Delta\omega_D$ is the Doppler linewidth, $\theta_0 << 1$ is the characteristic scattering angle. The calculation of the χ_{coll} is too difficult, so far as the parameters ν_{12}'' and θ_0 are known only by order of magnitude. One can resolve the elastic collisions contribution to the resonance asymmetry by analyzing the dependence of the modulation shift $\Delta\Omega$ on the deviation D. For the case of small asymmetry $\chi_{coll} << 1$ this dependence reads

$$\Delta\Omega = \chi_{coll}\frac{5}{2}\frac{(1+\sqrt{1+m^2})^3}{(1+3\sqrt{1+m^2})(1+m^2)^2}\Gamma. \tag{12}$$

One can see that the modulation shift $\Delta\Omega$ changes appreciably for $m \le 1$ in contrast to the lens shift (8), which changes appreciably for $m > 1$.

4.3. Modulation shifts measurements

For experimental investigations of the modulation shifts and the asymmetry of the resonances, the group of four HFS components of the absorption line of iodine (*d, e, f* and *g* components) was chosen. This choice was caused by the location of this group on the top of the gain curve of the lasers under investigation. Owing to this fact, the contribution of the Doppler curve of the gain line to the resonance asymmetry is minimal. The *d* component coincides with the center of the gain line. For *g* component, which is the most distant from the center of the gain line (approximately 40 MHz), the contribution of the Doppler curve to the modulation shift is not larger than 1 kHz [16].

Fig. 5 shows the measured dependencies of the frequency shift on the deviation D for the *d, e, f* and *g* components. The iodine cell cold-finger temperature was T=20°C, what corresponds to the iodine pressure of p = 27 Pa. The saturation of absorption is weak for this pressure. The low level of amplitude fluctuations in the He-Ne/$^{127}I_2$ lasers pumped by RFD enabled to measure the above mentioned dependencies in the range of deviation from D = 1.5 MHz to D = 20 MHz. One can see that the dependencies corresponding to different components diverge for the large deviation. It is caused by overlapping wings of the neighboring components.

The contribution of the overlapping wings to the total modulation shift can be evaluated exactly if the shape of the resonances is Lorentzian and their width is known. Since the saturation of absorption is weak the assumption about the Lorentzian shape of the resonances is valid. Thus, the laser output power curve can be expressed as [16]:

$$P(\omega) = P_0 \exp\left\{-\left(\frac{\omega-\omega_g}{\Delta\omega_D}\right)^2\right\} \times \left[1 + \sum_{i=1}^{4} k_i \frac{1}{1+(\Delta\omega_i/\Gamma_i)^2}\right], \tag{13}$$

where ω_g is the central frequency of the Doppler-broadened gain profile.

To obtain the parameters of the resonances we per-

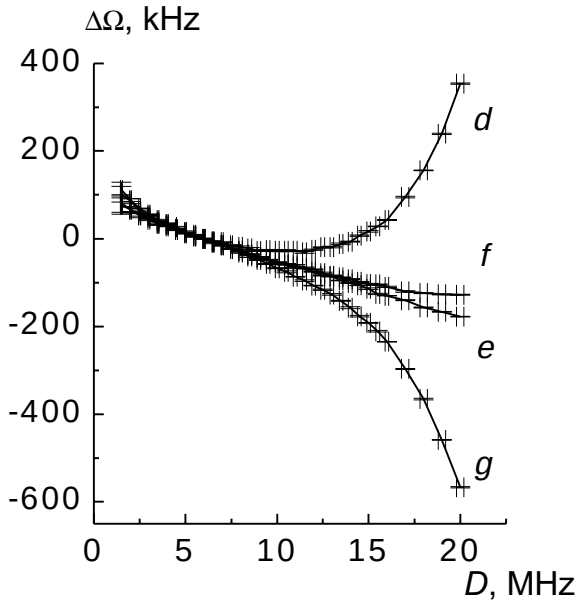

Fig. 5. Dependencies of the frequency shift on the frequency deviation for the *d, e, f* and *g* components.

formed a least-squares fit of the experimental dependencies of the third harmonic signals (in the vicinity of the *d, e, f* and *g* components) on the laser frequency to the theoretical ones given by formulae (7) and (13). The change of the laser frequency was measured by detecting a beat frequency between the laser under investigation and the reference laser. The last one was stabilized to one of the saturated absorption resonances. The parameters of the laser and the absorbing medium were the same as in the case of the modulation shifts measurement.

Fig. 6 shows two examples of the experimental data and the best analytic fit to these curves. As can be seen, the data are very well described by the expressions (7) with (13).

The least-squares fit gave, within the limits of error, the same values of the homogeneous width Γ_i and contrast k_i for all used values of deviation D and for all components. We obtained the value of Γ_i = 2.5±0.1 MHz and the frequency distances between components $\Delta\omega_{de}$= =12.9 ± 0.1 MHz, $\Delta\omega_{df}$= 26.2 ± 0.1 MHz, $\Delta\omega_{dg}$= = 39.4 ± 0.1 MHz.

The fact that least-squares parameters doesn't depend on the deviation D means that the model (13) used for the shape of the resonances is quite adequate, and it could be used for calculation of the frequency shifts caused by the overlapping wings relating to the neighboring components of the iodine HFS. Fig. 7 shows the results of the calculation for these shifts obtained by numerical solving the equation (6) for output power (13). One can see that the shift is maximal for outer components *d* and *g* and almost absent for the *f* component which is located approximately halfway between the *d* and *e* components. This fact provides that spurious contribution of the *d* and *e* components compensate each other.

Fig. 8 shows the results of the calculated shifts caused by the overlapping wings of the neighboring components subtraction from the total measured modulation shifts. One can see that the residual modulation shifts are the same within the limits of error for all four components. This fact verifies the validity of the model used for the description of the mutual influence of components. Thus, the residual shifts shown in the Fig. 8 can be attributed to the joint action of the gas-lens effect of the absorbing medium (8) and the elastic velocity-changing collisions of absorbing molecules (12). As can be seen, their dependence on the deviation D is substantially nonlinear. A least-squares fit of this dependence to the theoretical one given by the sum of formulae (8) and (12) leads to the following values of the asymmetry parameters χ_{lens} and χ_{coll} :

$$\chi_{lens} = -(5.2\pm0.2)\cdot10^{-2}; \qquad \chi_{coll} = (0.90\pm0.05)\cdot10^{-2}. \qquad (14)$$

The contributions of both asymmetry sources to the total modulation shift are shown in the Fig. 8. One can see that they are approximately equal for the deviation D = 6 MHz, which is recommended by BIPM for practical use.

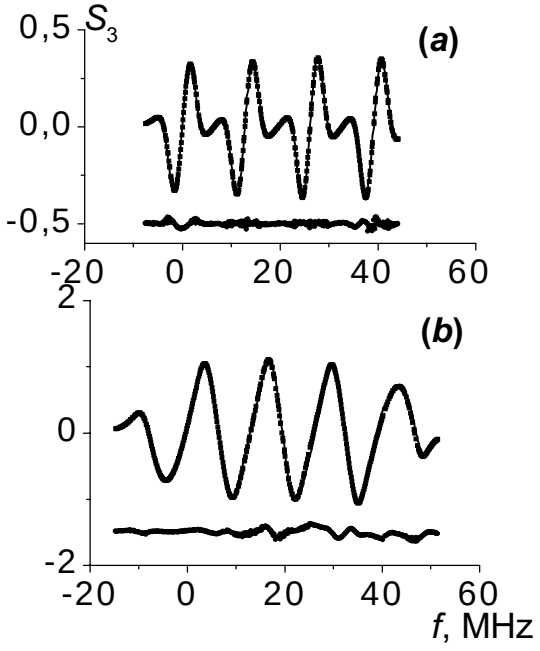

Fig. 6. Examples of fitting of the experimental data for third harmonic sygnal to the theoretical curves for D = 6 MHz (*a*) and D = 19 MHz (*b*). Circles are experimental data, the line is the result of fitting, and bottom circles are the difference between the experimental data and the fit (Γ = 2.5 MHz, $\Delta\omega_{de}$= =12.9 MHz, $\Delta\omega_{df}$= 26.2 MHz, $\Delta\omega_{dg}$= 39.4 MHz, k = 0.001).

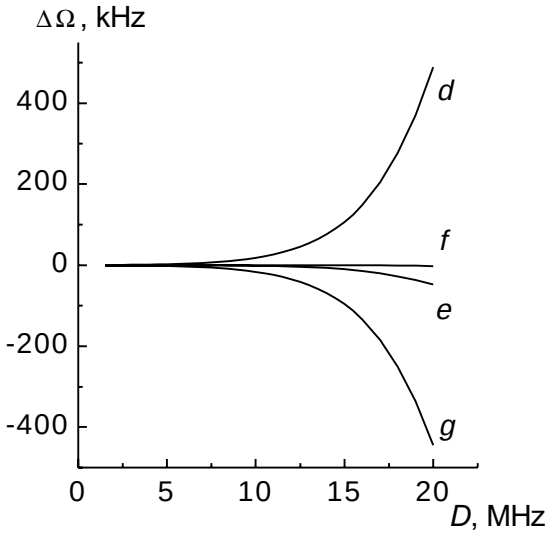

Fig. 7. Dependencies of the modulation shifts caused by the overlapping wings of the neighboring components of the iodine HFS on the deviation.

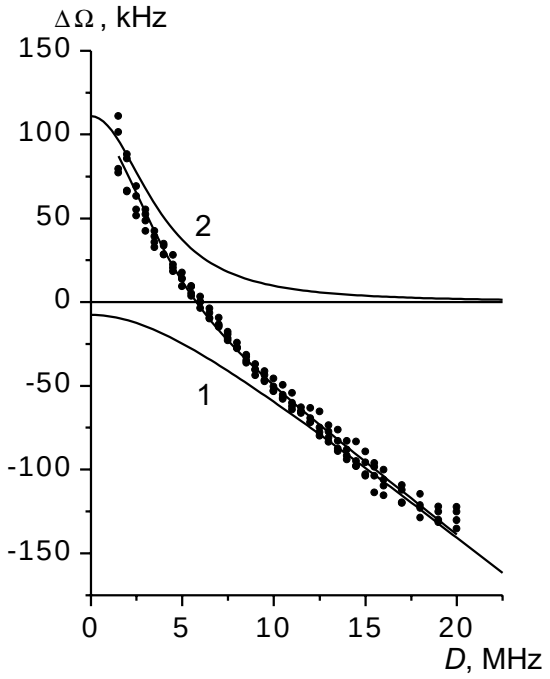

Fig. 8. The modulation shifts caused by the asymmetry of saturated-absorption resonances. Curve 1 correspondes to the lens effect, curve 2 correspondes to the elastic velocity-changing collisions of absorbing molecules.

5. Comparisons of lasers

The frequency of the developed laser (IP-2) was compared with the frequency of the laser DE-3 (Kharkiv) which is currently serving as part of the Ukrainian national length standard. The comparisons were carried out from 28 to 30 June 1998 at the Institute of physics of NAS of Ukraine.

The most important parameters of the lasers participating in the comparisons are summarized in table1.

The frequency difference between laser IP-2 and reference laser DE-3 was measured by the commonly used matrix measurement method [17]. The deviation and the iodine cell cold-finger temperature of the lasers were closely adjusted to the values recommended by the *mise en pratique* of the definition of the metre [2]. The iodine cell cold-finger temperature of the laser IP-2 was supported at 15.05 ± 0.01°C, and for DE-3 – 15.10 ± 0.01°C. The frequency deviation for the both lasers was $D = 6.0 \pm 0.1$ MHz. The beat-frequency record consisted of a matrix of measurements of frequency differences between the *d, e, f, g* HFS components excluding measurements of the main diagonal. For each matrix element the five successive beat-frequencies were measured for the integration time of 10 s, then the middle beat-frequencies f_{middle} and its standard uncertainties s were calculated.

$$f_{middle} = \frac{1}{n}\sum_{i=1}^{n} f_i , \tag{15}$$

$$s = \sqrt{\frac{\sum_{i=1}^{n}\left(f_{middle} - f_i\right)^2}{(n-1)}} \quad . \tag{16}$$

where n is a number of measurements of beat-frequency.

The frequency differences $\Delta f = f_{IP\text{-}2} - f_{DE\text{-}3}$ obtained versus current matrix number for laser IP-2 compared with laser DE-3 expressed as the results of sets of matrix determinations considering *d, e, f, g* HFS components are shown in the Fig. 9. The averaged frequency difference over the *d, e, f, g* absorption components was

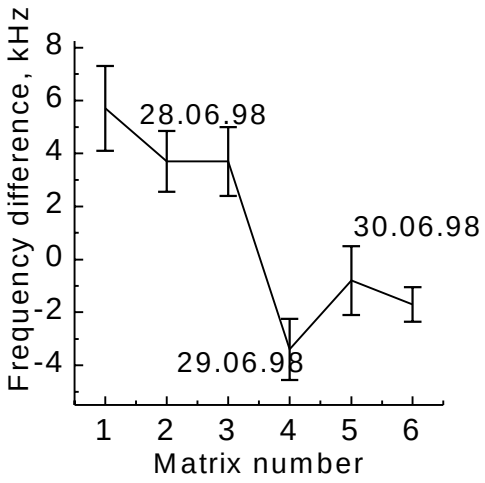

Fig. 9. The frequency differences obtained versus current matrix number for the laser IP-2 compared with the laser DE-3 expressed as the results of sets of matrix determinations considering *d, e, f, g* HFS components.

Table 1. The parameters of the lasers IP-2 and DE-3.

Laser	Cavity length, mm	Cell length, mm	Tube mirrors		Cell mirrors		Intracavity power, mW
			R1, mm	r1, %	R2, mm	r2, %	
IP-2	450	65	200	99.8	100	99.0	13
DE-3	230	65	100	99.7	100	99.0	5.2

$\Delta f = f_{IP-2} - f_{DE-3} = +1.2$ kHz,

with an estimation of the standard uncertainty $s = 3.2$ kHz.

The frequency stability was measured for the integration time 10 and 100 sec when lasers were stabilized by the *e* and *f* components. Calculating frequency stability, the Allan variance, $\sigma(2,\tau)$, was used. The results of these measurements are shown in table 2.

Table 2. The beat-frequency stability of the lasers IP-2 and DE-3.

τ, s	10	100
$\sigma(2, \tau)$	2.1×10^{-12}	7.9×10^{-13}

The frequency shift coefficients (for changing iodine cell cold-finger temperature $\Delta T(I_2)$, iodine vapor pressure $\Delta p(I_2)$ and deviation of frequency ΔD) of the laser IP-2 are given in table 3. The listed coefficients were calculated by least-squares linear fitting of the measurement data. The value of frequency deviation was varied in the range of 4 MHz < D < 8 MHz. The temperature of cold finger of the iodine cell was varied in the range of 12 °C < < T < 17 °C, which corresponded to changing iodine vapor pressure in the range of 13 Pa < p < 21 Pa.

6. Conclusions

The experimental investigations of the saturated-absorption resonances in the He-Ne/$^{127}I_2$ lasers pumped by transverse RFD were carried out. The high signal-to-noise ratio was obtained due to the low level of the amplitude fluctuations. The frequency stability of such lasers was about six times as large as the stability of the lasers pumped by DC-discharge. The modulation shifts of the frequency of stabilized He-Ne/$^{127}I_2$ lasers were measured with high accuracy in the wide range of the frequency deviation 1.5 MHz ≤ D ≤ 20 MHz. The sources of the asymmetry of saturated-absorption resonances were determined as the joint action of the lenslike properties of the absorption medium and the elastic velocity-changing collisions of absorbing molecules. The frequency of the developed laser was compared with the frequency of the laser DE-3 (Kharkiv) which is currently serving as a part of the Ukrainian national length standard. The measured frequency variation was 1.2 ± 3.2 kHz.

Acknowledgements

The autors wish to thank Lykholit M.M., Grinenko V.M., Khodakovskiy V.M. for their help during this work and Machekhin Yu.P., Smulakovskiy V.M. for participating in the comparisons of lasers.

This work was supported by grant 2M/1380-97-24 of Ministry of science and technologies of Ukraine and by project B15/24 of NAS of Ukraine.

References

1. Documents Concerning the New Definition of the Metre. // Metrologia. **19,** pp. 163-177 (1984).
2. Revision of the *mise en pratique* of the definition of the metre. *Recommendation adopted by the Comite International des Poids et Mesures at its 86th meeting*. Recommendation 1 (CI-1997).
3. J.-M.Chartier, J.Helmcke, A.J.Wallard, International intercomparison of the wavelength of iodine-stabilized lasers // *IEEE Inst.*

Table 3. Measured frequency shift coefficients of the laser IP-2. Laser DE-3 was taken as the reference. *s* represents estimation of the standard uncertainty.

		B	*s*
$(\Delta f/\Delta T(I_2))$/(kHz/°C)	*d*	-16.4	2.1
	e	-14.4	2.2
	f	-13.7	3.3
	g	-12.5	1.8
middle		-14.2	
s=		1.6	
$(\Delta f/\Delta p(I_2))$/(kHz/Pa)	*d*	-10.7	2.9
	e	-9.4	2.7
	f	-9.0	3.3
	g	-8.2	1.4
middle		-9.3	
s=		1.0	
$(\Delta f/\Delta D)$/(kHz/MHz)	*d*	-7.3	3.9
	e	-12.0	4.4
	f	-11.2	3.7
	g	-14.1	2.4
middle		-11.2	
s=		2.8	

Meas. **25**(4), pp. 450-453 (1976).
4. A.N.Titov, On the ultimate accuracy of the method of saturated absorption // *Quantum electronics* **8**(9), pp. 2039-2042 (1981).
5. P.Cerez, R.Felder, Gas-lens effect and cavity design of some frequency-stabilized He-Ne lasers // *Appl. Opt*. **22**(8), pp. 1251-1256, (1983).
6. D.N.Ghosh Roy, F.Bertinetto, B.I.Rebaglia, P.C.Cresto, Effects of iodine saturation dispersion on the stabilized He-Ne laser // *J. Appl. Phys*. **54**(2), 531-534 (1983).
7. Yu.M.Malyshev, Yu.G.Rastorguev, A.N.Titov, A shift in the frequency of lasers stabilized by the third harmonic due to the refractive index saturation // *Quantum electronics* **11**(6), pp. 1257-1260 (1984).
8. M.V.Danileyko, A.L.Kravchuk, A.M.Tselinko, L.P.Yatsenko, An asymmetry of nonlinear resonances and frequency shifts of stabilized He-Ne/$^{127}I_2$ lasers // *Quantum electronics* **13**(3), pp. 516-522 (1986).
9. J.-M.Chartier, A.Chartier, International comparisons of He-Ne lasers stabilized with $^{127}I_2$ at $\lambda \approx 633$ nm (July 1993 to September 1995) // *Metrologia* **34** , pp. 297-300 (1997).
10. Yu.P.Machekhin, V.A.Odinets, V.A.Smulakovskiy, Yu.S.Domnin, V.P.Tenishev, Comparisons of He-Ne/I_2 lasers maked by the program KOOMET 94/UA-a/92 in 1996 // *Izmeritelnaya tekhnika,* N11, pp. 71-72 (1997).
11. Ya.N.Muller, Use of gas microwave discharge in lasers // *Izv. Vuzov SSSR Ser. Radioelectronika* **22**(106), pp. 55-68 (1979).
12. Ya.N.Muller, V.M.Geller, V.A.Khrustalev, Use of transverse microwave discharge in a compact-efficient He-Ne laser // *Sov. J. Quantum electronics,* **9**(10), pp. 1302-1303 (1979).
13. V.M.Geller, G.I.Grif, V.A.Khrustalev, Use of transverse microwave discharge in helium-neon lasers // *Avtometria*, N1, pp. 35-45 (1984).
14. M.V.Danileyko, A.L.Kravchuk, A.M.Tselinko, L.P.Yatsenko, Helium-neon lasers stabilized by saturated absorption in iodine // *Quantum electronics*, Kiev, (36), pp. 1-20 (1989).
15. N.M.Danileyko, V.I.Romanenko, L.P.Yatsenko, Theory of the spatial inhomogeneity effects in gas lasers // *Preprint IF AN Ukrainy* N.21, Kiev, 1988, 38 p.
16. P.Cerez, A.Brillet, Factors which limit the reproducibility of iodine stabilized He-Ne lasers // *Metrologia,* **13**(1), pp. 29-33 (1977).
17. F.Bayer-Helms, J.-M.Chartier, J.Helmcke, A.J.Wallard, Evaluation of the International intercomparison measurements (March 1976) with $^{127}I_2$-stabilized He-Ne lasers. Spacing of the hyperfine structure components // *PTB-Berict* **PTB-ME17**, pp. 139-146 (1977).